MERCK

catch the SUN

Product Category list:

- Organic Photovoltaic (OPV) Donors and Acceptors
- Dye-Sensitized Solar Cell Materials
- Perovskite Materials

Visit us at:
SigmaAldrich.com/organic-electronics

MK_AD9792EN 43729 08/2022

The Life Science business of Merck operates as MilliporeSigma in the U.S. and Canada.

Sigma-Aldrich®
Lab & Production Materials

Energy Technology
Generation, Conversion, Storage, Distribution
www.entechnol.de

Synthesis and Application of an Aromatic Sulfonate Sodium Salt for Aqueous Sodium-Ion Battery Electrolytes

Xu Dong, Xu Liu, Jin Han, Zhen Chen, Huang Zhang, Stefano Passerini, and Dominic Bresser**

The two-step synthesis of sodium (2,3,5,6-tetrafluorophenoxy) diethane sulfonate (Na-TFP) is reported, starting from 2,3,5,6-tetrafluorohydroquinone as the precursor. Compared with conventional aqueous electrolytes such as 0.5 m $NaClO_4$ and Na_2SO_4, the 0.5 m aqueous solution of Na-TFP provides higher ionic conductivity over a wide range of temperature (e.g., >60 mS cm^{-1} at 20 °C and >70 mS cm^{-1} at 30 °C) and a wider electrochemical stability window. Electrochemical cells with $Na_2VTi(PO_4)_3$ as the positive electrode active material and a carbon-based negative electrode provide a stable capacity for more than 450 cycles in 0.5 m Na-TFP. Additionally, symmetric cells with $Na_2VTi(PO_4)_3$ as the active material for the negative and positive electrode are studied. The cells employing 0.5 m Na-TFP exhibit a good cycling stability at a high dis-/charge rate of 5C for more than 50 cycles, which is superior to the performance of the cells employing 0.5 m aqueous solutions of $NaClO_4$ and Na_2SO_4 as the electrolyte. The design of this bifunctional salt may trigger new ideas for the development of water-based sodium-ion battery electrolytes.

1. Introduction

Lithium-ion batteries (LIBs) are one of the major choices for energy storage in modern portable consumer electronics and electric vehicles.[1–4] However, concerning the enormous consumption and rising price of Li resources, new rechargeable battery systems beyond LIBs have recently drawn a lot of attentions.[5–7] Thanks to the high abundance of sodium and other raw materials employed, sodium-ion batteries (SIBs) are expected to offer lower costs than LIBs. Thus, they are emerging as a promising alternative.[8–10] In particular, aqueous sodium-ion batteries (ASIBs) with high safety and environmental friendliness are attractive candidates for next-generation rechargeable batteries.[11–13] Nonetheless, they also possess several shortcomings to be overcome. First, the electrochemical stability window (ESW) of the aqueous electrolytes with low salt concentration is rather narrow (≈1.23 V), which limits the voltage output and the choice of high-energy electrode materials of ASIBs.[14] Therefore, the overall energy density of ASIBs is much lower than the conventional nonaqueous LIBs.[14] Moreover, side reactions such as active material dissolution, anode passivation, and electrolyte decomposition can also reduce the reversibility and stability of ASIBs.[15]

As important components of SIBs, electrolytes have been extensively investigated.[16,17] Currently, there are a lot of efforts invested in the development of high-concentration electrolytes, i.e., "water-in-salt" electrolytes, to suppress the electrochemical decomposition of water, particularly, the hydrogen evolution reaction.[18–20] However, the high content of the salt increases the viscosity and decreases the ionic conductivity, which limits the rate capability of the aqueous cells.[21–23] Developing novel electrolyte salts for low concentration aqueous electrolytes with expanded ESW and high ionic conductivity is an interesting, alternative path for constructing ASIBs with superior cycle life, storage performance, and high-energy density.

Fluorinated organic compounds have been known for about two centuries, tracing back to 1835.[24] In 1929, the interest in this material class started blooming owing to the commercialization of nonflammable refrigerants such as CCl_3F and CCl_2F_2.[25] In Germany, the commercial production of aromatic fluorine compounds began in 1930, and numerous applications have surfaced in recent years. For example, fluoroaromatics have played an important role in the development of drugs and other products that are used as intermediates for pharmaceuticals and pesticides.[26,27] Substituted hexafluorobenzene compounds found potential use in optical applications and as photoresists,[28] as complexing agent for transition metals in catalysis.[29,30] More recently, they have been proposed also as redox-active component in the catholyte of redox-flow batteries.[31] While there are generally a lot of studies on the nucleophilic substitution of halide groups and phenols,[32–37] little and only rather fundamental studies have been reported on the investigation of 2,3,5,6-tetrafluorohydroquinone, also referred to as perfluorobiphenol.[38–40] However, the rather pronounced intermolecular interaction potential in combination with the facile modification of the

X. Dong, X. Liu, J. Han, Z. Chen, H. Zhang, S. Passerini, D. Bresser
Helmholtz Institute Ulm (HIU)
89081 Ulm, Germany
E-mail: dominic.bresser@kit.edu; stefano.passerini@kit.edu

X. Dong, X. Liu, J. Han, Z. Chen, H. Zhang, S. Passerini, D. Bresser
Karlsruhe Institute of Technology (KIT)
76021 Karlsruhe, Germany

The ORCID identification number(s) for the author(s) of this article can be found under https://doi.org/10.1002/ente.202201045.

DOI: 10.1002/ente.202201045

two hydroxyl groups, opening up the potential for the synthesis of bifunctional alkali metal salts, render it a very interesting starting block for the synthesis of novel electrolyte salts.

In this work, we propose sodium (2,3,5,6-tetrafluorophenoxy) diethane sulfonate (Na-TFP) as a new conducting salt for aqueous electrolytes. Even with a low salt concentration, i.e., 0.5 m, its aqueous solution not only realizes a wider ESW but also exhibits a higher ionic conductivity with respect to the conventional Na_2SO_4 and $NaClO_4$ containing electrolytes. As a result, the symmetric NVTP cells comprising the 0.5 m Na-TFP electrolyte exhibit higher specific capacity and better cyclability than those employing the Na_2SO_4 and $NaClO_4$ electrolytes.

2. Results and Discussion

Na-TFP was synthesized using perfluorobiphenol as the precursor following a two-step derivatization (**Figure 1**). The first step consists of a nucleophilic substitution of perfluorobiphenol (**1**) by 1,2-dibromoethane under basic conditions,[41] followed by the sulfoethylation reaction with Na_2SO_3 to yield sodium sulfonate groups in the second step.[34] The chemical structure of the intermediate (**2**) and the final product Na-TFP (**3**) were confirmed by ^{1}H NMR, ^{19}F NMR, ^{13}C NMR, and FT-IR spectroscopy (see Figure S1–S3, Supporting Information). Subsequently, we investigated the potential application of Na-TFP as conducting salt in aqueous electrolytes for sodium-ion batteries (SIBs), a battery technology that has recently attracted a lot of interest for large-scale stationary applications, owing to the abundancy of its constituents and potentially low cost.[5,42–44] Aqueous electrolytes are particularly attractive for stationary storage applications because of their intrinsic safety and high ionic conductivity, while the limited electrochemical stability of water and, thus, the limited cell voltage is less of an issue, as the weight and volume of the battery are not very detrimental. In fact, the ionic conductivity of the aqueous 0.5 m Na-TFP electrolyte (0.5 mol Na-TFP in 1 kg water) is as high as 45 mS cm^{-1} at 10 °C, >60 mS cm^{-1} at 20 °C, >70 mS cm^{-1} at 30 °C, and 115 mS cm^{-1} at 60 °C (**Figure 2**a). This is significantly higher than the conductivity of 0.5 m aqueous solutions of $NaClO_4$ and Na_2SO_4 with, for instance, only 41 and 51 mS cm^{-1} at 20 °C for $NaClO_4$ and Na_2SO_4, respectively. For the determination of the ESW, three-electrode cells employing a platinum working electrode, activated carbon (AC) counter electrode, and Ag/AgCl reference electrode were assembled and subjected to linear sweep voltammetry (LSV) (Figure 2b). At a first glance, the ESW appears rather wide with about 2.5 V in between the sharp rise of the cathodic and anodic current. However, a closer inspection indicates that the perfectly flat region is limited to about −0.6 V upon reduction and 0.6 V upon oxidation, with a minor increase in current beyond these values, which is in good agreement with the theoretically expected ESW of water of about 1.2 V prior to hydrogen and oxygen evolution upon reduction and oxidation, respectively.[45] When comparing the ESW of the Na-FTP electrolyte with those based on $NaClO_4$ and Na_2SO_4, however, it is observed that especially the stability toward reduction appears superior for Na-TFP, while the stability toward oxidation is higher than for Na_2SO_4 and comparable to $NaClO_4$.

The potential use of the salt in aqueous electrolytes for SIBs was further studied in combination with NVTP as the electrode

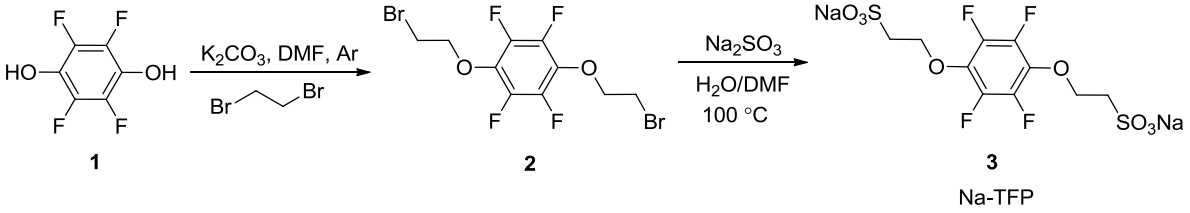

Figure 1. Synthesis procedure for yielding the bifunctional sodium salt Na-TFP (**3**), starting from 2,3,5,6-tetrafluoro-hydroquinone (**1**) as the precursor.

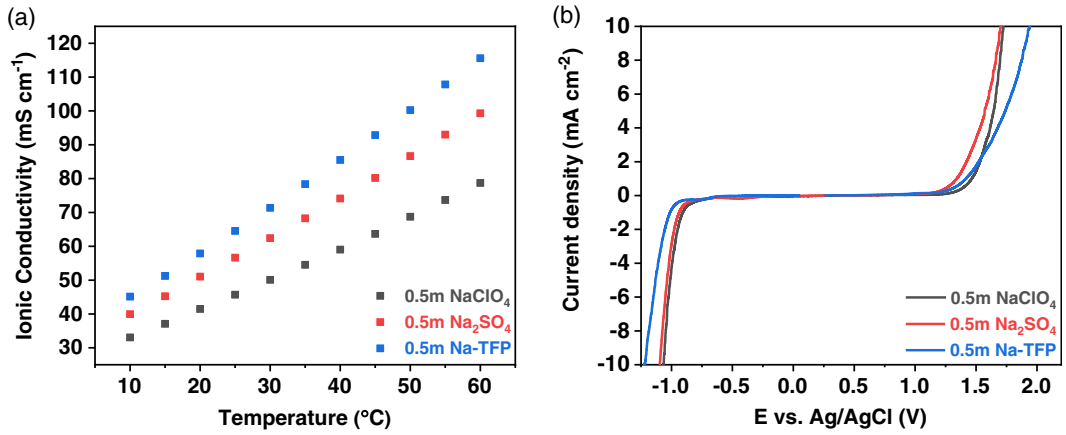

Figure 2. Electrochemical characterization of the 0.5 m aqueous solutions of $NaClO_4$, Na_2SO_4, and Na-TFP: a) Ionic conductivity as a function of temperature; b) Determination of the electrochemical stability window by means of LSV at 20 °C and a sweep rate of 10 mV s^{-1}.

active material, which has been reported earlier as very suitable for aqueous SIBs[46–49] and AC as the counter electrode.[50] The determination of the crystal structure by X-ray diffraction (XRD; Figure S4, Supporting Information) revealed a phase-pure material, and the analysis of the morphology via scanning electron microscopy (SEM) coupled with energy-dispersive X-ray spectroscopy (EDX; Figure S5, Supporting Information) showed a particle size of several micrometers and a homogeneous distribution of oxygen, vanadium, sodium, and titanium in the sample – in line with the previous study.[51]

In a first step, the potential range for the V^{3+}/V^{4+} redox couple in NVTP was investigated, and the cut-off potentials were set to 0.0 and 0.6 V versus Ag/AgCl (**Figure 3**a,b and S6a,b, Supporting Information), i.e., toward the upper stability limit of the electrolyte. The comparison of the three electrolytes reveals a (slightly) higher specific capacity for the NVTP||AC cells comprising the Na-TFP electrolyte at all C rates. Especially, the $NaClO_4$-based electrolyte provides a relatively limited capacity at elevated C rates (Figure S6a, Supporting Information) compared to the other two electrolyte systems. The average Coulombic efficiency was about 99.8% for all electrolytes, indicating a generally sufficient stability in this potential range. This is also reflected by the very stable long-term cycling of such cells in the given potential range with a capacity retention of about 90% after more than 400 cycles at 2C in the case of Na-TFP following the evaluation of the rate capability (Figure 3a). The capacity retention of the Na_2SO_4-based electrolyte was about 92%, while it was somewhat lower for the $NaClO_4$-based electrolyte (86%). The dis-/charge profiles of all three electrolytes show the characteristic potential plateau at about 0.4 V (Figure 3b and S6a,b, Supporting Information). The reversible specific capacity at 2C was 46 mAh g^{-1} for Na-TFP and slightly decreased to 43 and 38 mAh g^{-1} when increasing the C rate to 5C and 10C, respectively, along with a slight increase in polarization. For the Na_2SO_4 electrolyte, the capacity was comparable with 43, 40, and 37 mAh g^{-1} at 2C, 5C, and 10C, respectively, while it was substantially lower for $NaClO_4$ with only 42, 36, and 23 mAh g^{-1} at the same C rates. The better rate capability offered by the Na-TFP-based electrolyte with respect to that achieved for the Na_2SO_4 and $NaClO_4$ electrolytes is ascribed to the superior ionic conductivity of the former electrolyte, as shown in Figure 2a.

In a second step, the potential range for the Ti^{3+}/Ti^{4+} redox couple in NVTP was studied (Figure 3c,d and S6c,d, Supporting Information). Therefore, the cut-potential values were set to −0.1 and −0.88 V versus Ag/AgCl. The use of the Na-TFP-based electrolyte leads to a remarkably improved specific capacity accompanied by higher Coulombic efficiency. This performance can be explained by the better cathodic stability of the Na-TFP-based electrolyte in comparison to the $NaClO_4$ and Na_2SO_4 comprising electrolytes, as demonstrated in Figure 2b. Nonetheless, the

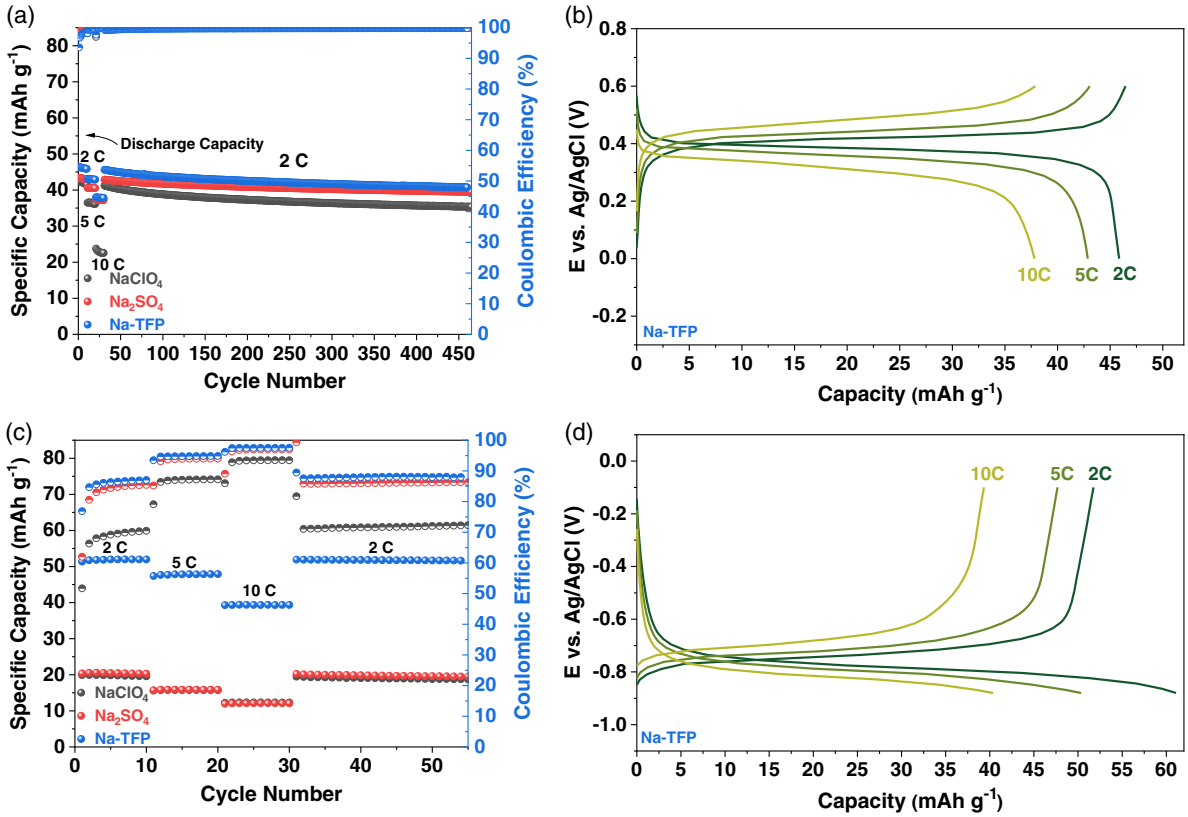

Figure 3. Galvanostatic cycling of electrochemical cells comprising NVTP as active material for the working electrodes and AC-based counter electrodes at varying C rates in a potential range from a,b) 0.0 to 0.6 V and c,d) −0.1 to −0.88 V versus Ag/AgCl: a,c) Comparison of the rate capability and cycling stability of the NVTP||AC cells comprising the three different electrolytes; b,d) selected dis-/charge profiles of the NVTP||AC cell containing the Na-TFP-based electrolyte at varying C rates, i.e., 2C (dark green), 5C (green), and 10C (light green).

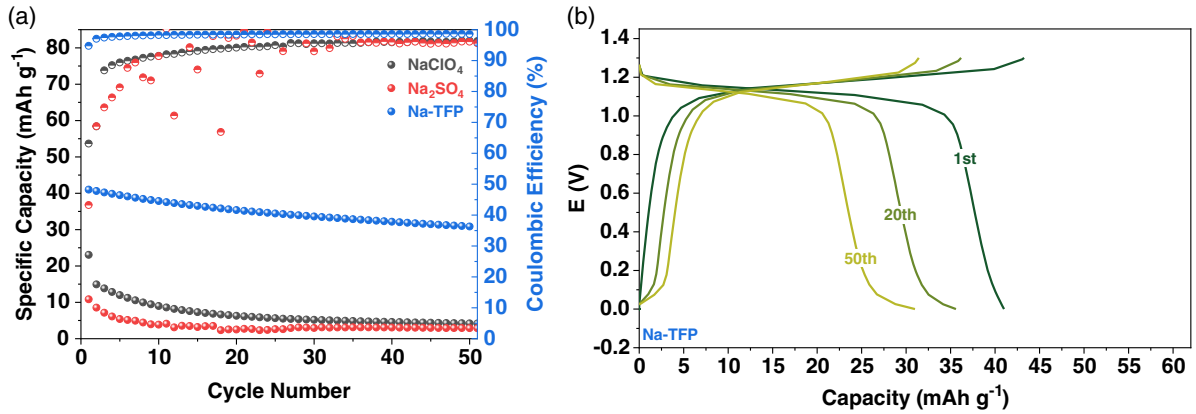

Figure 4. Galvanostatic cycling of symmetric NVTP||NVTP cells at 5C: a) comparison of the cycling stability and Coulombic efficiency of the three different electrolyte systems; b) selected dis–/charge profiles for the 1st, 20th, and 50th cycle of the NVTP||NVTP cell comprising the Na-TFP electrolyte.

Coulombic efficiency for Na-TFP electrolyte remains rather low at 2C with less than 90%, despite an increase to 94.9% at 5C and 97.9% at 10C (Figure 3c). Further improvement of the cathodic stability of the proposed electrolyte is still required to suppress the hydrogen evolution reactions for a better reversibility. Nonetheless, the cycling stability appears very promising with no significant capacity fading (Figure 3c), revealing that the active material itself is not the cause of the limited Coulombic efficiency, while there is apparently an excess of electrolyte in the cell and a minor hydrogen evolution does not affect the overall performance. The dis–/charge profiles of Na-TFP presented in Figure 3d show the typical potential plateau at around −0.75 V and a promising specific capacity of about 52 mAh g^{-1} at 2C, which decreases to 48 and 39 mAh g^{-1} when increasing the dis-/charge rate to 5C and 10C, respectively. For $NaClO_4$ and Na_2SO_4, the reversible capacities are much lower with only 20/20, 16/16, and 12/12 mAh g^{-1} ($NaClO_4$/Na_2SO_4) at 2C, 5C, and 10C, respectively, accompanied by a slightly (Na_2SO_4) and substantially ($NaClO_4$) lower Coulombic efficiency (Figure 3c and S6c,d, Supporting Information).

Finally, symmetric NVTP||NVTP cells were assembled and subjected to galvanostatic cycling at 5C in a voltage range from 0.0 to 1.3 V (**Figure 4** and S7, Supporting Information). In such case, the two earlier studied redox reactions occur simultaneously at the negative and positive electrodes. The cells employing $NaClO_4$ or Na_2SO_4 as the conducting salt exhibit a very abrupt fading after the first cycle and very poor specific capacities, rapidly approaching 4 mAh g^{-1}. This is accompanied by very low Coulombic efficiencies caused by the insufficient reversibility of the Ti^{3+}/Ti^{4+} redox couple in the Na_2SO_4 and $NaClO_4$ electrolytes. In comparison, the specific capacity of the NVTP||NVTP cell comprising the Na-TFP-based electrolyte was substantially higher with initially more than 40 mAh g^{-1}, highlighting the very good rate capability of such electrodes and the Na-TFP-based aqueous electrolyte. Benefiting from the extended cathodic stability and, especially, high ionic conductivity, the specific capacity delivered by the 0.5 m Na-TFP electrolyte at high specific currents, e.g., 5C, is also superior to those obtained with the reported highly concentrated electrolytes, e.g., 9.2 m $NaCF_3SO_3$, 8 m $NaClO_4$,[48] 8 m CH_3COONa, and 32 m CH_3COOK + 8 m CH_3COONa.[52] Moreover, about 75% of this specific capacity, i.e., 30 mAh g^{-1}, were retained after 50 cycles. The average Coulombic efficiency was 98.6% – in line with the previous findings, confirming the superior performance of the Na-TFP electrolyte.

3. Conclusion

Sodium (2,3,5,6-tetrafluorophenoxy) diethane sulfonate (Na-TFP) was successfully synthesized as new bifunctional sodium battery electrolyte salt via a facile two-step derivatization starting from the commercially available 2,3,5,6-tetrafluorohydroquinone (perfluorobiphenol). Compared with equimolal aqueous $NaClO_4$ and Na_2SO_4 electrolytes, this new sodium salt shows a higher ionic conductivity of, e.g., >70 mS cm^{-1} at 30 °C, which translates into an enhanced rate capability of $Na_2VTi(PO_4)_3$ electrodes for both the V^{3+}/V^{4+} and the Ti^{3+}/Ti^{4+} redox couple, as evaluated in NVTP||AC cells. Additionally, the electrochemical stability toward reduction is substantially enhanced, resulting in the superior capacity and cycling stability of symmetric NVTP||NVTP cells. In sum, the results show that Na-TFP is a suitable electrolyte salt for ASIBs and potentially also for other electrolyte media.

4. Experimental Section

Materials and Synthesis: 2,3,5,6-Tetrafluorohydroquinone (Alfa Aesar, >96%), 1,2-dibromoethane (Sigma–Aldrich, >98%), *N,N*-dimethylformamide (DMF, Alfa Aesar, >99.8%), anhydrous potassium carbonate (Alfa Aesar, >99%), and purified sodium sulfite (VWR, 95.0–100.5%) were used as received. Following the study by Wang et al.,[41] a solution of 2,3,5,6-tetrafluorohydroquinone (**1**) (4.0 g, 21.1 mmol) in 10 mL DMF was added dropwise to a continuously stirred mixture of 1, 2-dibromoethane (15.8 g, 84.4 mmol) and K_2CO_3 (8.7 g, 63.2 mmol) in DMF (40 mL) at room temperature, as depicted later. After the addition had been completed, the reaction mixture was stirred at room temperature for another 2 h and then heated to 70 °C for 2 h. The mixture was filtered, and the resulting solution was diluted with ethyl acetate (80 mL) and washed three times with 80 mL H_2O. The organic layer was separated, dried with anhydrous Na_2SO_4, and concentrated under reduced pressure

to give **2** (7.4 g, yield: 89%). ^{1}H, ^{19}F, and ^{13}C NMR spectra of 2 are provided in Figure S1, Supporting Information and were recorded on a Bruker AM-400 spectrometer.

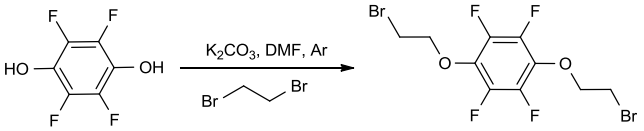

1 **2**

^{1}H NMR (400 MHz, $CDCl_3$) $\delta = 4.46$–4.39 (t, $J = 6.4$ Hz, 4H), 3.65 – 3.58 (t, $J = 6.4$ Hz, 4H); ^{19}F NMR (400 MHz, $CDCl_3$) $\delta = -155.10$ (s, Ar-F).

Subsequently, according to Sigwalt et al.,[34] a solution of **2** (5.2 g, 13.1 mmol) and Na_2SO_3 (3.7 g, 28.7 mmol) in H_2O/DMF (1:1, 120 mL) was prepared under nitrogen atmosphere and stirred at 100 °C for 24 h. Afterward, the mixture was cooled naturally to room temperature and filtered. The filtrate was poured into acetone (1 L) and the precipitate was collected by filtration and dried on the filter funnel overnight. The crude solid was dissolved in boiling water (15 mL) and EtOH (120 mL) was added to precipitate the product. The mixture was cooled naturally to room temperature and filtered. The resulting white solid yielded the final product **3** after drying under high vacuum (4.3 g, yield: 80%). ^{1}H, ^{19}F, and ^{13}C NMR spectra of **3** are displayed in Figure S2, Supporting Information. An FT-IR spectrum, recorded using a Bio-Rad Excalibur FT-IR spectrometer in the 400–4000 cm^{-1} wavenumber range, is presented in Figure S3, Supporting Information and compared with the FT-IR spectrum of **2**.

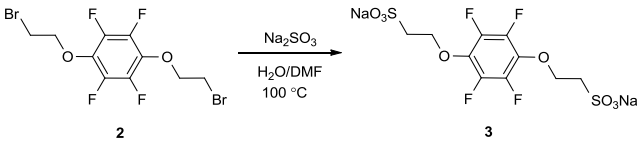

2 **3**
Na-TFP

^{1}H NMR (400 MHz, DMSO) $\delta = 4.39$–4.31 (m, 4H), 2.98–2.86 (m, 4H); ^{19}F NMR (400 MHz, DMSO) $\delta = -157.93$ (s, Ar-F). IR (KBr): $\nu = 3620$, 3546, 2970, 1613, 1504, 1426, 1389, 1300, 1211, 1169, 1055, 987, 934, 809, 637, 585, 522 cm^{-1}.

Electrochemical Characterization of the Na-TFP-Based Electrolyte: The aqueous electrolyte comprising Na-TFP as the final product was prepared by dissolving 0.5 mol of the salt in 1 kg of deionized water. 0.5 m was the highest concentration that Na-TFP can achieve in water. At this level, further decreasing the salt concentration leads to lower ionic conductivity and narrower ESW. Thus, we selected 0.5 m as the concentration to comprehensively and comparatively investigate the physical and electrochemical properties. Accordingly, 0.5 m solutions of $NaClO_4$ (Sigma–Aldrich, 99.99%) and Na_2SO_4 (Merck KGaA, >99%) were prepared. The ionic conductivity of the different electrolyte systems was determined in sealed conductivity glass cells (AMEL 192/K1), equipped with two porous platinum electrodes. The cell constants were determined using a 0.01 M KCl standard solution. The measurements were run in the temperature range from 10 to 60 °C, and the equilibration time at each temperature was 1 h. The ESW of the electrolyte solutions was determined by LSV at 20 °C on a multichannel potentiostat/galvanostat (VMP, BioLogic), using three-electrode Swagelok-type cells and applying a sweep rate of 10 mV s^{-1}. Platinum disk (1 mm in diameter), AC (YP-47, Kuraray), and Ag/AgCl electrodes were used as working, counter, and reference electrode, respectively.

Electrode Preparation, Cell Assembly, and Testing: $Na_2VTi(PO_4)_3$ (NVTP) was synthesized by a sol–gel method.[51] In brief, 0.02 mol $CH_3COONa{\cdot}3H_2O$ (VWR, >99%), 0.01 mol NH_4VO_3 (Sigma–Aldrich, >99%), and 0.03 mol $NH_4H_2PO_4$ (Alfa Aesar, >99%) were dissolved in 50 mL of an aqueous solution of citric acid monohydrate ($C_6H_8O_7{\cdot}H_2O$) (0.02 M; Alfa Aesar, >99%). Under vigorous stirring, 10 mL of a 0.1 M solution of $Ti(CH_3CH_2CH_2CH_2O)_4$ (Sigma–Aldrich, >98%) in absolute ethanol (VWR, >99.9%) were added to the former solution. The slightly yellowish solution turned immediately into a white suspension. After heating this suspension to 80 °C to evaporate the solvents, the resulting blue powder was collected as the gel precursor. The precursor was pretreated at 350 °C for 5 h and then sintered at 800 °C for 12 h under argon flow to obtain the NVTP electrode active material. X-ray diffraction (XRD) was carried out using a Bruker D8 with a Cu–Kα radiation source ($\lambda = 0.154$ nm). The morphology of the NVTP powder was investigated by SEM utilizing a ZEISS EVO MA 10 microscope, equipped with an EDX detector (Oxford Instruments X-MaxN, 50 mm^2, 15 kV).

The electrodes were composed of 80 wt% NVTP or AC (YP-47, Kuraray) as the active material, 10 wt% SuperC65 (Imerys) as conductive additive, and 10 wt% polyvinylidene difluoride (Solef 6020, Solvay) as binder.[52] The latter was dissolved in *N*-methyl-2-pyrrolidone (anhydrous, Sigma–Aldrich) before adding the other electrode components. The resulting slurry was dispersed using a ball milling machine (Pulverisette 4, Fritsch) for 2 h and cast on battery grade stainless steel. After drying at 80 °C overnight, disk-shaped electrodes with a diameter of 12 mm were punched and further dried at 120 °C under high vacuum. The average active material mass loading was about 3.0 mg cm^{-2}. When combining NVTP as the working electrode and AC as the counter electrode, three-electrode Swagelok-type cells were used, comprising additionally a Ag/AgCl reference electrode. In the case of the symmetric NVTP||NVTP cells, two-electrode CR2032 coin cells were assembled with the weight ratio of the active materials close to 1. In both cases, glass fiber sheets (GF/D, Whatman) served as separator and were soaked with the aqueous electrolyte. Galvanostatic cycling was conducted on a Maccor 4000 Battery Test System. A C rate of 1C refers to a specific current of 100 mA g^{-1}. All electrochemical tests were conducted at 20 °C.

Supporting Information

Supporting Information is available from the Wiley Online Library or from the author.

Acknowledgements

The authors would like to acknowledge financial support from the Federal Ministry of Education and Research (BMBF) within the FestBatt project (03XP0175B) and the HyPerium project (03XP0403C) as well as from the Helmholtz Association.

Open Access funding enabled and organized by Projekt DEAL.

Conflict of Interest

The authors declare no conflict of interest.

Data Availability Statement

The data that support the findings of this study are available on request from the corresponding author. The data are not publicly available due to privacy or ethical restrictions.

Keywords

conducting salts, electrolytes, sodium vanadium phosphate, sodium-ion batteries, symmetric cells

Received: September 8, 2022
Revised: October 12, 2022
Published online:

[1] L. Qiu, M. Zhang, Y. Song, Y. Xiao, Z. Wu, W. Xiang, Y. Liu, G. Wang, Y. Sun, J. Zhang, *EcoMat* **2021**, *3*, e12141.
[2] Z. Ye, B. Zhang, T. Chen, Z. Wu, D. Wang, W. Xiang, Y. Sun, Y. Liu, Y. Liu, J. Zhang, *Angew. Chem.* **2021**, *133*, 23436.
[3] Z. Yang, T. Chen, D. Chen, X. Shi, S. Yang, Y. Zhong, Y. Liu, G. Wang, B. Zhong, Y. Song, *Angew. Chem., Int. Ed.* **2021**, *60*, 12539.
[4] L. Ni, R. Guo, S. Fang, J. Chen, J. Gao, Y. Mei, S. Zhang, W. Deng, G. Zou, H. Hou, *eScience*, **2022**, *2*, 116.
[5] B. Dunn, H. Kamath, J.-M. Tarascon, *Science* **2011**, *334*, 928.
[6] M. M. Thackeray, C. Wolverton, E. D. Isaacs, *Energy Environ. Sci.* **2012**, *5*, 7854.
[7] H. Xue, H. Gong, Y. Yamauchi, T. Sasaki, R. Ma, *Nano Res. Energy* **2022**, *1*, 9120007.
[8] L. Wang, Z. Huang, B. Wang, G. Liu, M. Cheng, Y. Yuan, H. Luo, T. Gao, D. Wang, R. Shahbazian-Yassar, *ACS Appl. Mater. Interfaces* **2019**, *11*, 10663.
[9] V. Palomares, P. Serras, I. Villaluenga, K. B. Hueso, J. Carretero-González, T. Rojo, *Energy Environ. Sci.* **2012**, *5*, 5884.
[10] T. Liu, B. Wang, X. Gu, L. Wang, M. Ling, G. Liu, D. Wang, S. Zhang, *Nano Energy* **2016**, *30*, 756.
[11] M. K. Khoshkbarchi, J. H. Vera, *Ind. Eng. Chem. Res.* **1996**, *35*, 2735.
[12] Y. You, Z. Sang, J. Liu, *Mater. Technol.* **2016**, *31*, 501.
[13] Y. Wang, L. Mu, J. Liu, Z. Yang, X. Yu, L. Gu, Y. S. Hu, H. Li, X. Q. Yang, L. Chen, *Adv. Mater.* **2015**, *5*, 1501005.
[14] H. Che, S. Chen, Y. Xie, H. Wang, K. Amine, X.-Z. Liao, Z.-F. Ma, *Energy Environ. Sci.* **2017**, *10*, 1075.
[15] H. Zhang, X. Tan, H. Li, S. Passerini, W. Huang, *Energy Environ. Sci.* **2021**, *14*, 5788.
[16] A. Ponrouch, E. Marchante, M. Courty, J.-M. Tarascon, M. R. Palacin, *Energy Environ. Sci.* **2012**, *5*, 8572.
[17] Y. Huang, L. Zhao, L. Li, M. Xie, F. Wu, R. Chen, *Adv. Mater.* **2019**, *31*, 1808393.
[18] L. Suo, O. Borodin, T. Gao, M. Olguin, J. Ho, X. Fan, C. Luo, C. Wang, K. Xu, *Science* **2015**, *350*, 938.
[19] M. R. Lukatskaya, J. I. Feldblyum, D. G. Mackanic, F. Lissel, D. L. Michels, Y. Cui, Z. Bao, *Energy Environ. Sci.* **2018**, *11*, 2876.
[20] T. Liu, L. Tang, H. Luo, S. Cheng, M. Liu, *Chem. Commun.* **2019**, *55*, 12817.
[21] J. Chen, J. Vatamanu, L. Xing, O. Borodin, H. Chen, X. Guan, X. Liu, K. Xu, W. Li, *Adv. Mater.* **2020**, *10*, 1902654.
[22] M. Yu, Y. Lu, H. Zheng, X. Lu, *Chem. A Eur. J.* **2018**, *24*, 3639.
[23] Q. Dou, S. Lei, D.-W. Wang, Q. Zhang, D. Xiao, H. Guo, A. Wang, H. Yang, Y. Li, S. Shi, *Energy Environ. Sci.* **2018**, *11*, 3212.
[24] R. Banks, J. Tatlow, *J. Fluorine Chem.* **1986**, *33*, 71.
[25] T. Midgley Jr, A. L. Henne, *Ind. Eng. Chem.* **1930**, *22*, 542.
[26] V. H. Mai, G. I. Nikonov, *ACS Catal.* **2016**, *6*, 7956.
[27] A. Arévalo, A. Tlahuext-Aca, M. Flores-Alamo, J. J. García, *J. Am. Chem. Soc.* **2014**, *136*, 4634.
[28] H. V. Tran, R. J. Hung, T. Chiba, S. Yamada, T. Mrozek, Y.-T. Hsieh, C. R. Chambers, B. P. Osborn, B. C. Trinque, M. J. Pinnow, *Macromolecules* **2002**, *35*, 6539.
[29] A. B. Chaplin, J. F. Hooper, A. S. Weller, M. C. Willis, *J. Am. Chem. Soc.* **2012**, *134*, 4885.
[30] E. Clot, O. Eisenstein, N. Jasim, S. A. Macgregor, J. E. McGrady, R. N. Perutz, *Acc. Chem. Res.* **2011**, *44*, 333.
[31] A. N. Jansen, J. T. Vaughey, Z. Chen, L. Zhang, F. R. Brushett, Google Patents **2016**.
[32] P. R. Ashton, R. Ballardini, V. Balzani, E. C. Constable, A. Credi, O. Kocian, S. J. Langford, J. A. Preece, L. Prodi, E. R. Schofield, *Chem. A Eur. J.* **1998**, *4*, 2413.
[33] R. Ayothi, Y. Yi, H. B. Cao, W. Yueh, S. Putna, C. K. Ober, *Chem. Mater.* **2007**, *19*, 1434.
[34] D. Sigwalt, D. Moncelet, S. Falcinelli, V. Mandadapu, P. Y. Zavalij, A. Day, V. Briken, L. Isaacs, *ChemMedChem* **2016**, *11*, 980.
[35] W.-K. Han, H.-X. Zhang, Y. Wang, W. Liu, X. Yan, T. Li, Z.-G. Gu, *Chem. Commun.* **2018**, *54*, 12646.
[36] H. Oh, K. Xu, H. D. Yoo, D. S. Kim, C. Chanthad, G. Yang, J. Jin, I. A. Ayhan, S. M. Oh, Q. Wang, *Chem. Mater.* **2016**, *28*, 188.
[37] S. Butini, M. Brindisi, S. Gemma, P. Minetti, W. Cabri, G. Gallo, S. Vincenti, E. Talamonti, F. Borsini, A. Caprioli, *J. Med. Chem.* **2012**, *55*, 6898.
[38] R. Sirutkaitis, P. Adomenas, in *Advances in Liquid Crystal Research and Applications*, Elsevier, Amsterdam **1981**, pp. 1023–1028.
[39] A. Kovács, I. Macsári, I. Hargittai, *J. Phys. Chem. A* **1999**, *103*, 3110.
[40] J. Lombard, T. le Roex, D. A. Haynes, *Cryst. Growth Des.* **2020**, *20*, 7384.
[41] W. Wang, C. Sheng, X. Che, H. Ji, Y. Cao, Z. Miao, J. Yao, W. Zhang, *Bioorg. Med. Chem. Lett.* **2009**, *19*, 5965.
[42] H. Kim, J. Hong, K.-Y. Park, H. Kim, S.-W. Kim, K. Kang, *Chem. Rev.* **2014**, *114*, 11788.
[43] D. Bin, F. Wang, A. G. Tamirat, L. Suo, Y. Wang, C. Wang, Y. Xia, *Adv. Mater.* **2018**, *8*, 1703008.
[44] T. Jin, X. Ji, P. F. Wang, K. Zhu, J. Zhang, L. Cao, L. Chen, C. Cui, T. Deng, S. Liu, *Angew. Chem., Int. Ed.* **2021**, *60*, 11943.
[45] D. M. Santos, C. A. Sequeira, J. L. Figueiredo, *Quim. Nova* **2013**, *36*, 1176.
[46] E. Gu, J. Xu, Y. Du, X. Ge, X. Zhu, J. Bao, X. Zhou, *J. Alloys Compd.* **2019**, *788*, 240.
[47] H. Wang, T. Zhang, C. Chen, M. Ling, Z. Lin, S. Zhang, F. Pan, C. Liang, *Nano Res.* **2018**, *11*, 490.
[48] H. Zhang, S. Jeong, B. Qin, D. Vieira Carvalho, D. Buchholz, S. Passerini, *ChemSusChem* **2018**, *11*, 1382.
[49] L. Shen, H. Yang, Y. Jiang, J. Ma, T. Sun, M. Zhang, N. Zhu, *ACS Sustainable Chem. Eng.* **2021**, *9*, 3490.
[50] M. Keller, T. Eisenmann, D. Meira, G. Aquilanti, D. Buchholz, D. Bresser, S. Passerini, *Small Methods* **2019**, *3*, 1900239.
[51] D. Wang, X. Bie, Q. Fu, D. Dixon, N. Bramnik, Y.-S. Hu, F. Fauth, Y. Wei, H. Ehrenberg, G. Chen, *Nat. Commun.* **2017**, *8*, 15888.
[52] J. Han, M. Zarrabeitia, A. Mariani, Z. Jusys, M. Hekmatfar, H. Zhang, D. Geiger, U. Kaiser, R. J. Behm, A. Varzi, *Nano Energy* **2020**, *77*, 105176.